Electronic Supplementary Material (ESI) for ChemComm.

Electronic Supplementary Information

Piezo-photocatalytic reduction of nitrates to N_2 over silver dispersed on $BaTiO_3$@TiO_2

Hongjie Luo,[a] Guoqiang Shu,[a,c] Shanhong Guo,[a] Xia Kuang,[a] Changming Zhao,[c] Chang-An Zhou,[a] Chao Wang,[a] Lei Song,[a] Kui Ma,*[a] and Hairong Yue[a,b]

a. Low-Carbon Technology and Chemical Reaction Engineering Laboratory, School of Chemical Engineering, Sichuan University, Chengdu 610065, China.

b. Institute of New Energy and Low-Carbon Technology, Sichuan University, Chengdu 610207, China.

c. Daqing Oilfield Production Technology Institute, Daqing 163453, China.

*Corresponding author: kuima@scu.edu.cn;

TEL/FAX: (+86) 28-85465318

Supplementary Experimental Section

1. Catalysts preparation

Synthesis of BTO nanoparticles. BTO was synthesized using a sol-gel hydrothermal method. Initially, 5 mL of deionized water and 5 mL of ethanol were added to a 50 mL round-bottom flask containing 8.5 mL of titanium butoxide, followed by the addition of 4 mL of ammonia solution at 80°C under magnetic stirring. This resulting solution was labeled as Solution A. Simultaneously, 11.83 g of barium hydroxide octahydrate was dissolved in 35 mL of deionized water to form a homogeneous solution under magnetic stirring at 80°C, and this solution was labeled as Solution B. Next, Solution B was added to Solution A and vigorously stirred for 20 minutes at 80°C. The final suspension was transferred to a 100 mL Teflon-lined autoclave and maintained at 200°C for 24 hours. Afterward, it was cooled to room temperature. The resulting product was washed several times with DI water and ethanol, followed by drying in a 60°C oven for 10 hours.[1]

Synthesis of BTO@TO core-shell material. BTO@TO nanoparticles were synthesized using a simple chemical bath method. Firstly, 0.2 M boric acid and 0.075 M ammonium fluoride titanium completely dissolved in 100 mL of DI water. The previously synthesized BTO nanoparticles were added to this solution and stirred at 60°C for 20 minutes, 40 minutes, 60 minutes, 80 minutes, and 120 minutes, respectively. The resulting products were washed several times with DI water and ethanol, followed by drying in a 60°C oven for 10 hours. The dried products were then heated in a muffle furnace with a heating rate of 1°C/min and maintained at 350°C for 30 minutes to obtain the final products. Based on the chemical bath time, the final products were designated as BTO@TO-20, BTO@TO-40, BTO@TO-60, BTO@TO-80, and BTO@TO-120.

Synthesis of Ag/BTO@TO. Different deposition concentrations of Ag/BTO@TO catalysts were synthesized using a deposition-precipitation method. Initially, 0.3g of BTO@TO nanoparticles were dispersed in 80 mL of DI water and sonicated for 5

minutes. While continuously stirring, 20 mL of anhydrous methanol was added. Subsequently, 473 μL, 1420 μL, and 2367 μL of 10 mg/mL $AgNO_3$ solution were separately added. Next, the pH was adjusted to 10 by adding 0.1 mol/mL NaOH solution dropwise, followed by 10 minutes of sonication and 30 minutes of continuous stirring. The resulting products were washed several times with DI water and ethanol, then dried in a vacuum oven at 40°C for 10 hours. The final products were labeled as Ag_1/BTO@TO, Ag_2/BTO@TO, and Ag_3/BTO@TO. The entire process was conducted in a dark environment.

2. Characterization

The X-ray diffraction (XRD) was tested by an XRD-6100 X-ray diffractometer (Shimadzu Corporation, Kyoto, Japan) with Cu–Ka beam source in 2θ at 10–90° range. A JEM-F200 (JEOL, Tokyo, Japan) transmission electron microscopy (TEM) was used to gain the TEM and high-resolution TEM (HRTEM) images of catalysts. X-ray photoelectron spectroscopy (XPS) was characterized by a K-Alpha (Thermo Scientific, Waltham, MA, USA) photoelectron spectrometer to detect the chemical state of the catalysts, and the element binding energy was corrected using the C1s peak at 284.80 eV. The UV-vis diffuse-reflectance spectra (UV-vis DRS) of as-prepared samples was performed with a UV-3600i Plus (Shimadzu Corporation, Kyoto, Japan) spectrometer equipped with an integrating sphere by using $BaSO_4$ as reference in the range of 200–800 nm. Photocurrent measurements were carried out on CHI 660E electrochemical workstation (Chenhua, Shanghai, China). A three-electrode battery made of nanostructured materials on FTO was used as the working electrode, and saturated Ag/AgCl and platinum electrodes were used as the counter electrode and reference electrode, respectively. The electrochemical impedance spectroscopy (EIS) tests were characterized over a 10^{-2} to 10^6 Hz frequency range. The Electron spin resonance (ESR) spectra were obtained by MS-5000X (Magnettech, Berlin, Germany) to detect $\cdot CO_2^-$,·OH and $\cdot O_2^-$ radicals using 5, 5-dimethyl-1-pyrroline-1-oxide (DMPO) as spin trap.

3. Catalyst activity testing

The prepared catalyst's piezo-photocatalytic activity was evaluated by the degradation of NO_3^- under the combined action of light and ultrasound. In this experiment, 50 mg of the catalyst was added to a 50 mL solution of $NaNO_3$ in water (50 mg/L), along with 100 µL of HCOOH. The mixture was stirred in the dark for 30 minutes to achieve adsorption-desorption equilibrium between the solvent and the catalyst. The reactor we used for catalytic activity testing is equipped with a circulation cooling water system to ensure the reactor and the solution temperatures maintain ~22-25 °C during the testing. Before each testing, reactor was evacuated and purged with argon gas for three cycles. Then, the ultrasound with 20 kHz and a 300 W xenon lamp were turned on to initiate the catalytic reaction. At specific time intervals, 1 mL of the suspension was withdrawn, centrifuged, and the concentrations of the NO_3^-, NO_2^-, and NH_4^+ products were analyzed using the ion chromatography (CIC-D100, SHINE, China). Based on this, we used nitrogen balance method to calculate the N_2 yield, which is generally accepted in photocatalytic nitrates reduction system. The corresponding calculation equations are described as follows:

$$X_{NO_3^-} = \frac{C_{NO_{3i}^-} - C_{NO_{3t}^-}}{C_{NO_{3i}^-}} \times 100\% \quad \text{(eq. S1)}$$

$$S_{NO_2^-} = \frac{C_{NO_{2t}^-}}{C_{NO_{3i}^-} - C_{NO_{3t}^-}} \times 100\% \quad \text{(eq. S2)}$$

$$S_{NH_4^+} = \frac{C_{NH_{4t}^+}}{C_{NO_{3i}^-} - C_{NO_{3t}^-}} \times 100\% \quad \text{(eq. S3)}$$

$$S_{N_2} = 1 - S_{NO_2^-} - S_{NH_4^+} \quad \text{(eq. S4)}$$

Where C_i and C_t represent the concentration of nitrogen species at irradiation time 0 and t, respectively. In order to confirm N_2 production, the gas phase product was collected and injected into a gas chromatograph (GC2060, Sanlikeji, China) to

detect N_2.

4. The formula for calculating the energy band structure

$$(\alpha h\nu)^{\frac{1}{n}} = B(h\nu - E_g) \quad \text{(eq. S5)}$$

$$h\nu = 1240/\lambda \quad \text{(eq. S6)}$$

$$E_g = E_{VB} - E_{CB} \quad \text{(eq. S7)}$$

where E_g represents the energy band width of the semiconductor, ν represents the frequency, h represents Planck's constant, B is a constant, α represents the absorption coefficient, n represents the index associated with the semiconductor, λ represents the wavelength, E_{VB} represents the valence band position, and E_{CB} represents the conduction band position.

Supplementary Figures

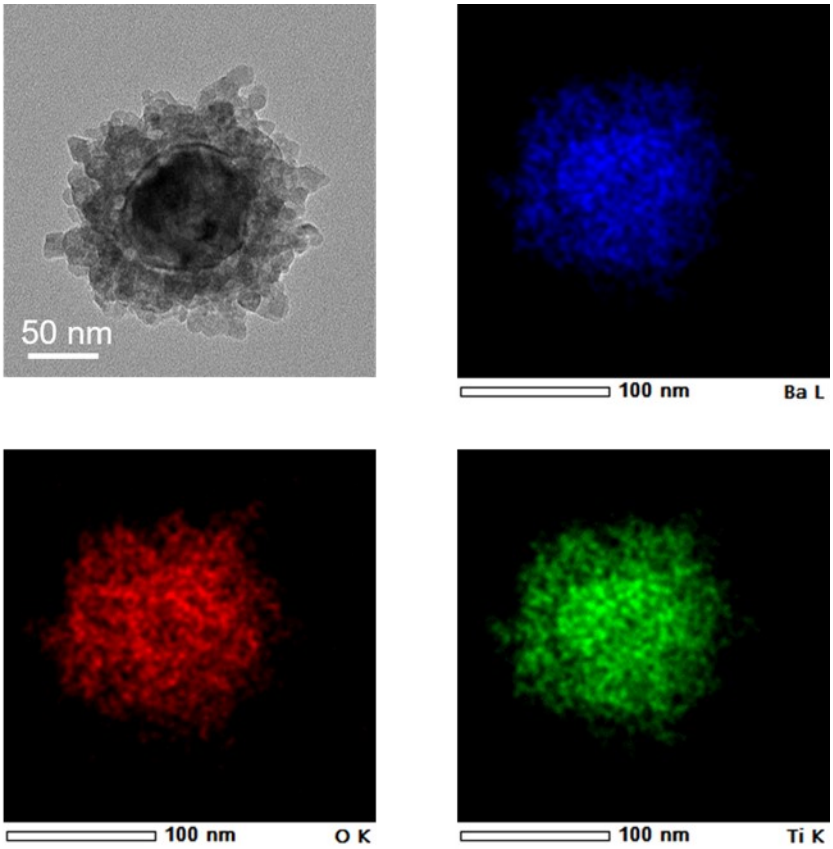

Figure S1. TEM-EDS elemental mapping of BTO@TO-40.

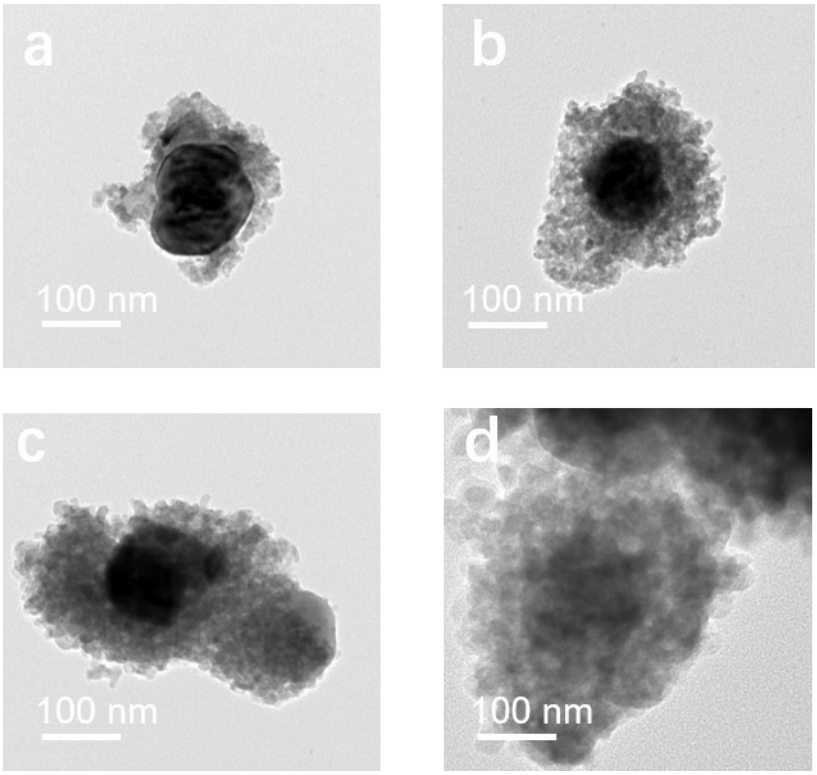

Figure S2. (a) TEM image of BTO@TO-20; (b) TEM image of BTO@TO-60; (c) TEM image of BTO@TO-80; (d) TEM image of BTO@TO-120.

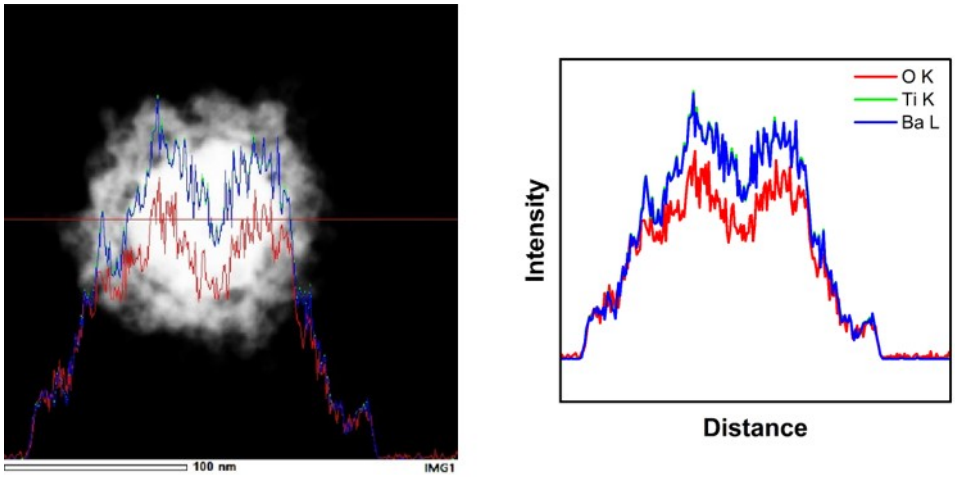

Figure S3. EDS line scan of BTO@TO-40.

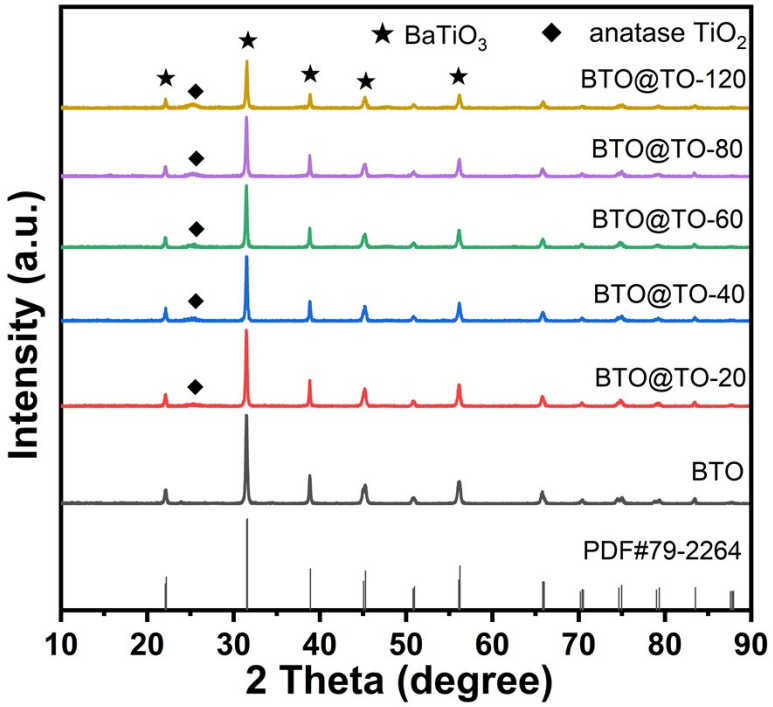

Figure S4. XRD spectra of BTO@TO with different chemical bath times.

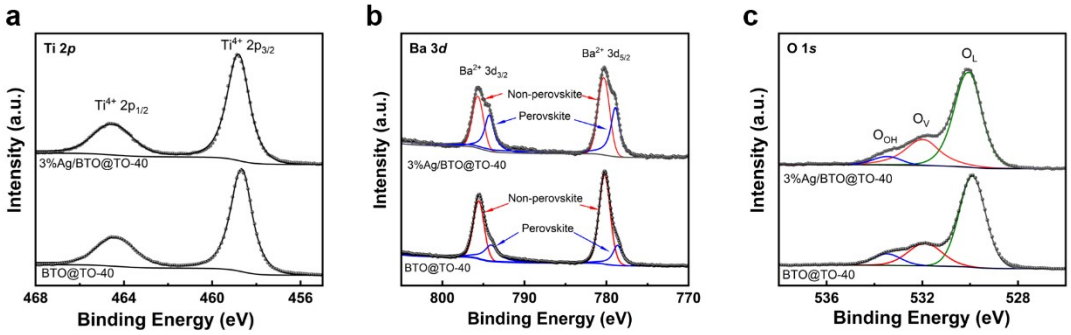

Figure S5. High-resolution XPS spectra of (a) Ti $2p_{1/2}$ and Ti $2p_{3/2}$, (b) Ba $3d_{5/2}$ and Ba $3d_{3/2}$, (c) O 1*s* in Ag_2/BTO@TO-40.

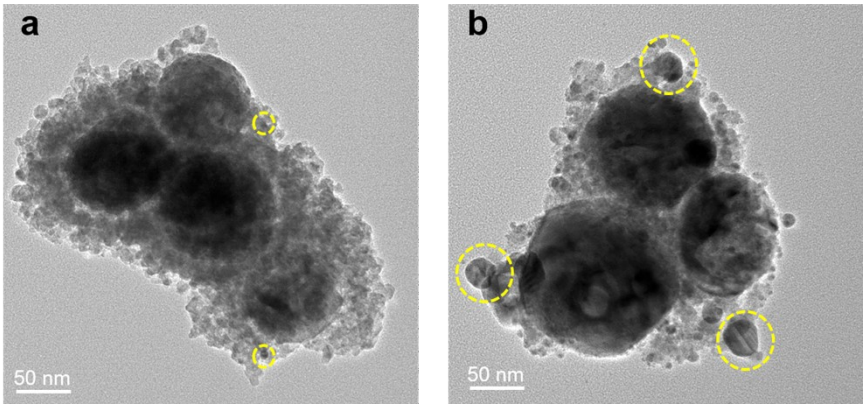

Figure S6. TEM images of (a) Ag_1/BTO@TO-40 and (b) Ag_3/BTO@TO-40.

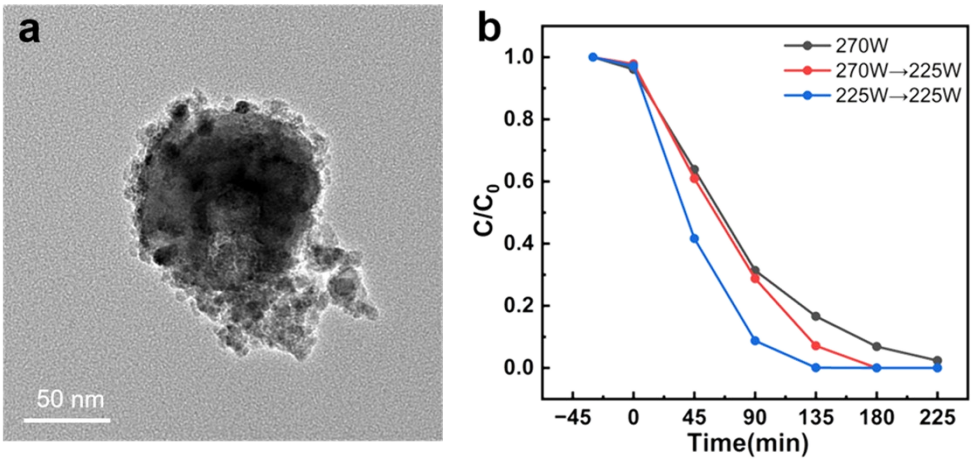

Figure S7. (a) TEM image of Ag_2/BTO@TO-40 after the reaction at 270 W; (b) Piezo-photocatalytic nitrates reduction activity of Ag_2/BTO@TO-40 under the condition of resetting the ultrasonic power to 225 W from 270 W.

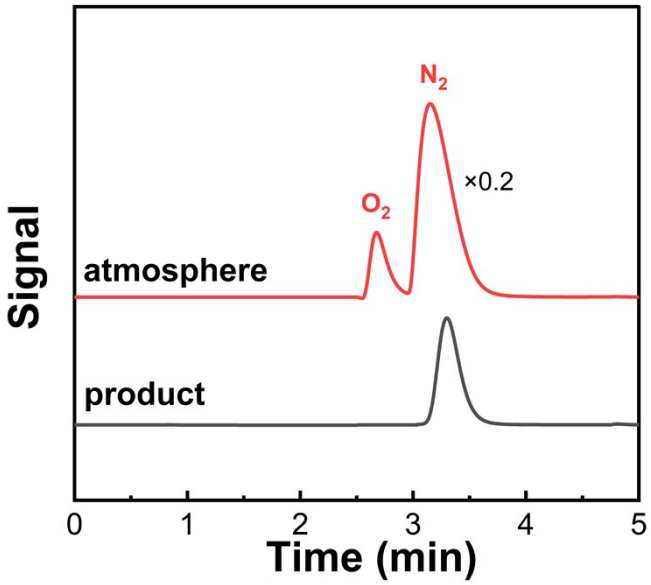

Figure S8. GC spectra of atmosphere and gas phase product of piezo-photocatalytic nitrates reduction over Ag_2/BTO@TO-40.

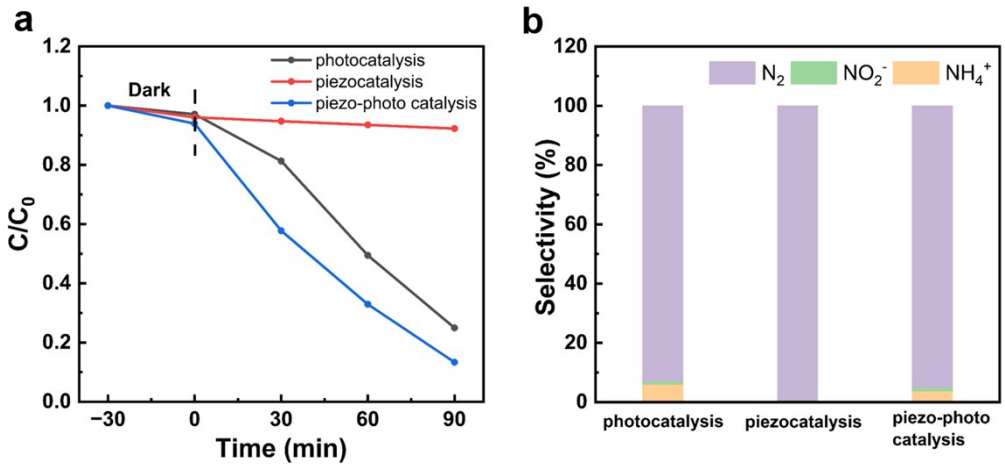

Figure S9. The photocatalytic, piezo-catalytic and piezo-photocatalytic (a) nitrates reduction activity and (b) the corresponding product selectivity over Ag_2/BTO@TO-40.

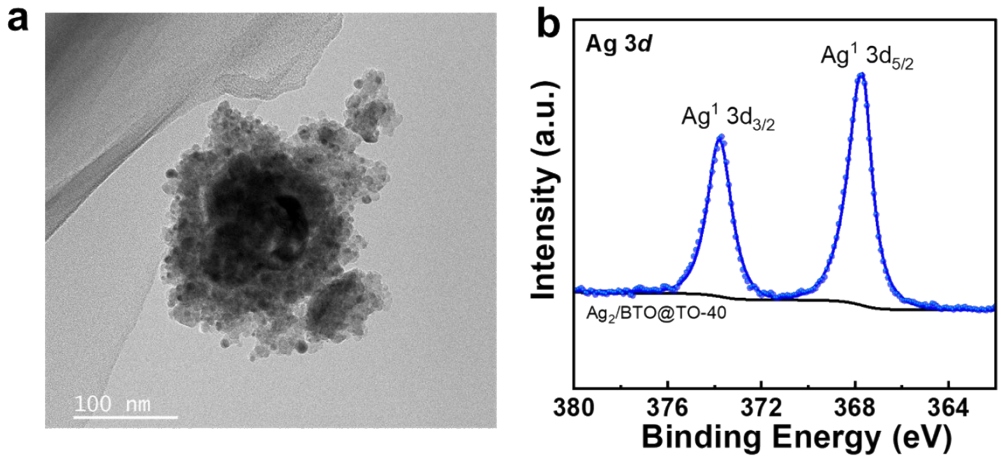

Figure S10. (a) TEM image and (b) Ag 3*d* XPS spectra of Ag_2/BTO@TO-40 after cycling experiment.

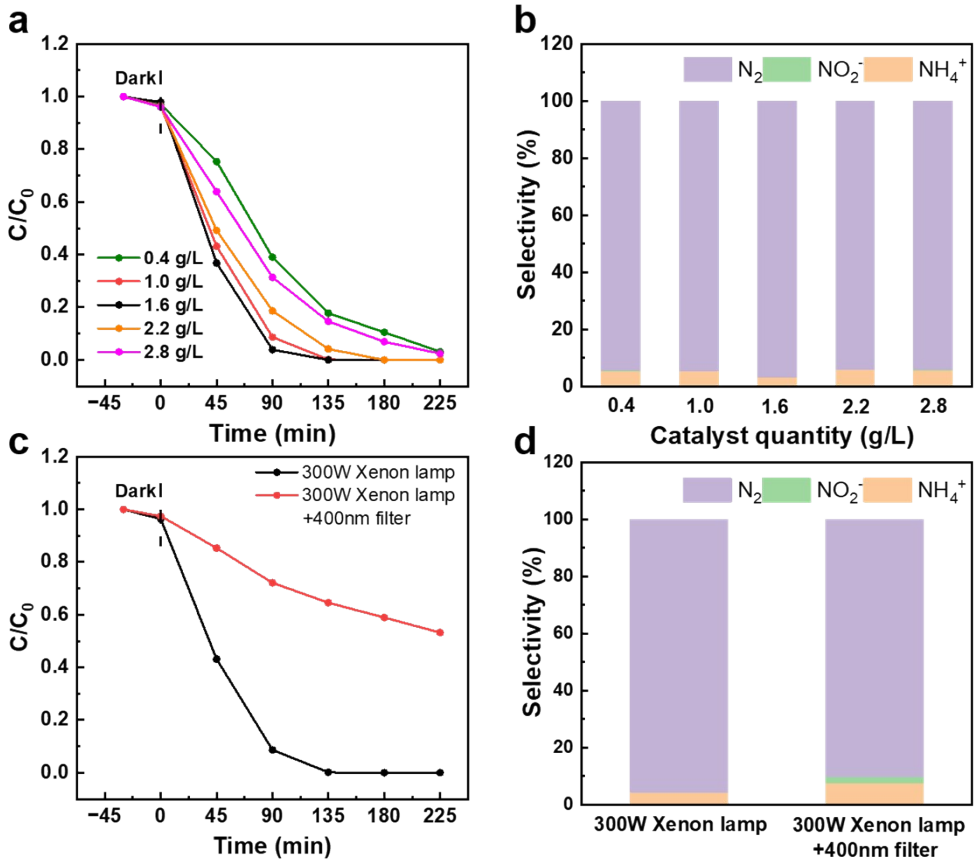

Figure S11. The effect of catalyst amount on piezo-photocatalytic activity (a) and products selectivity (b) over Ag_2/BTO@TO-40; The effect of light source on piezo-photocatalytic activity (c) and products selectivity (d) over Ag_2/BTO@TO-40.

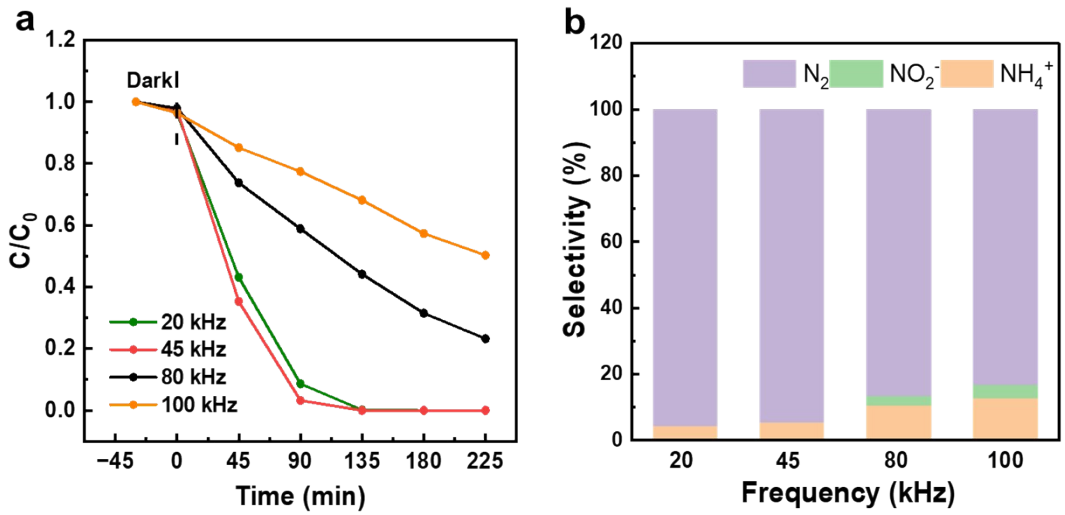

Figure S12. The effect of ultrasonic frequency on (a) piezo-photocatalytic activity and (b) products selectivity over Ag_2/BTO@TO-40.

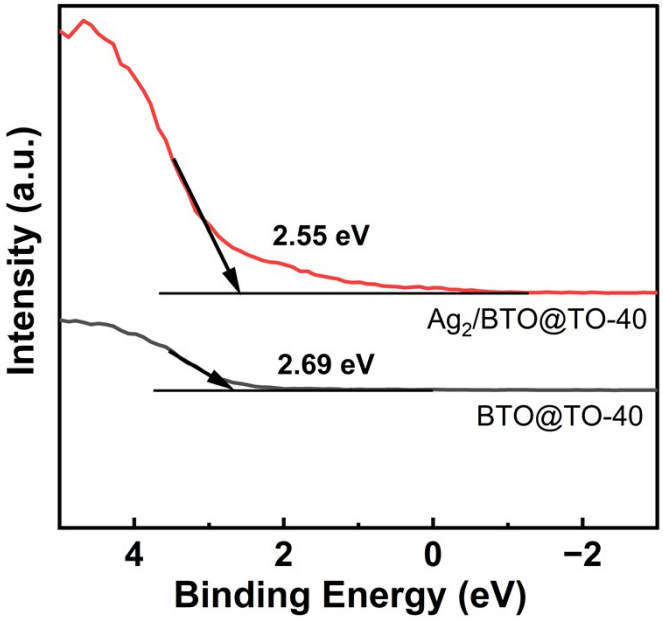

Figure S13. XPS-VB spectra of BTO@TO-40 and Ag_2/ BTO@TO-40.

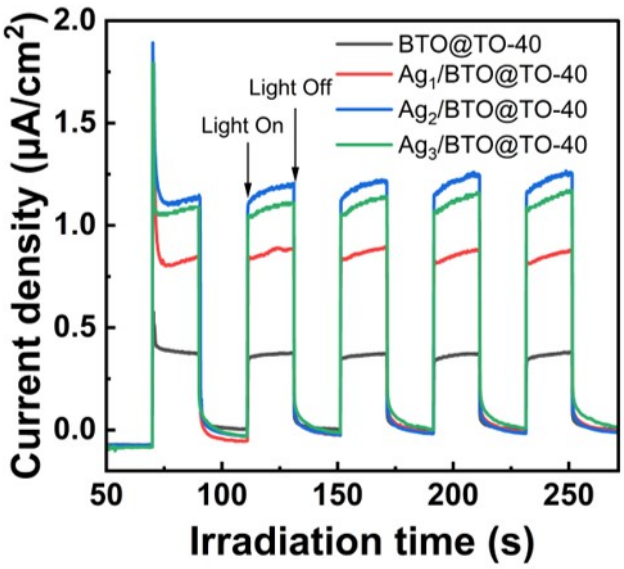

Figure S14. Photocurrent density curves for BTO@TO with different silver deposition.

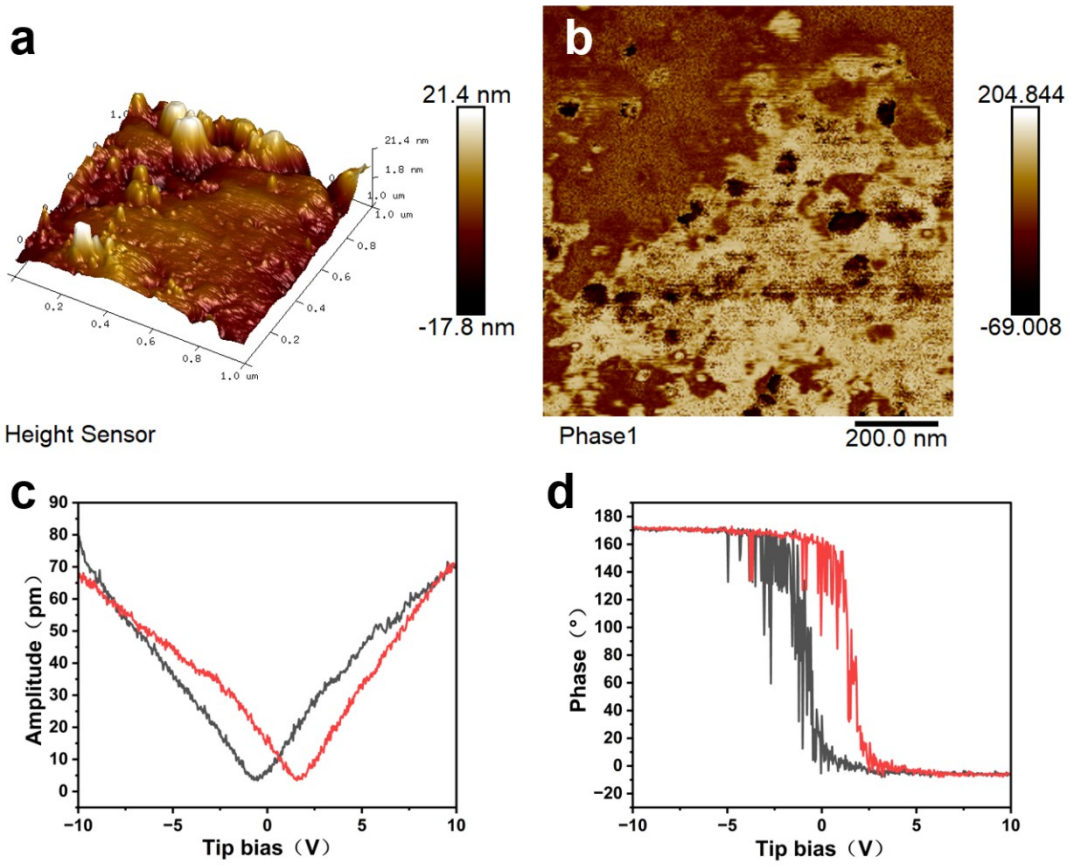

Figure S15. PFM tests of Ag_2/BTO@TO-40: (a) Topography image, (b) Phase image, (c) Amplitude butterfly loops and (d) Phase hysteresis loops.

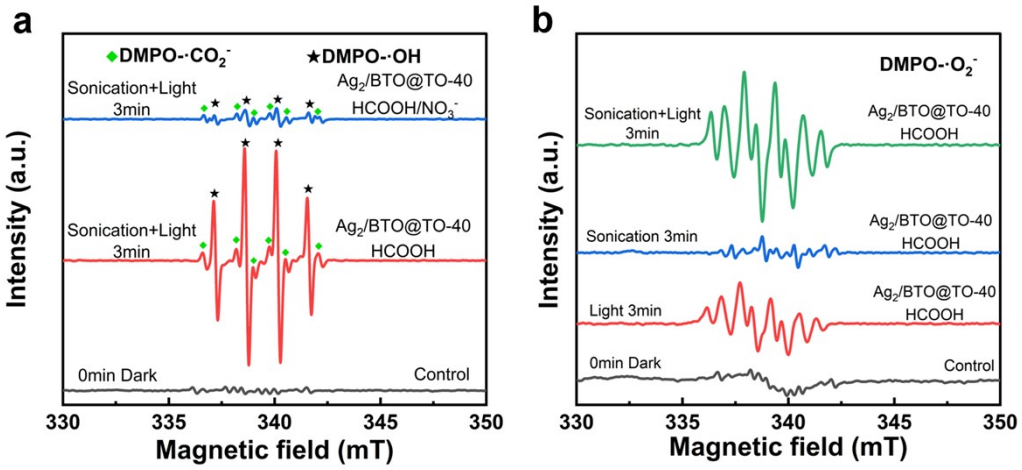

Figure S16. ESR spectra of Ag_2/BTO@TO-40: (a) $\bullet CO_2^-$ and •OH, (b) $\bullet O_2^-$.

Supplementary References

1. X. Huang, K. Wang, Y. Wang, B. Wang, L. Zhang, F. Gao, Y. Zhao, W. Feng, S. Zhang and P. Liu, *Appl. Catal. B Environ.*, 2018, **227**, 322-329.